The Indonesian Journal of Geography, Vol. 17, No. 54
December 1987, pp. 55—79.

OPERATIONAL PROCEDURE FOR MONITORING REMOTELY SENSED SEA SURFACE TEMPERATURES

by
Gastellu-Etchegorry J.P.,
Boely T.,
Christophil M.*

ABSTRACT

In Indonesia, there is now no operational sea surface temperature (SST) monitoring for such activities as oceanography, climatology or fishery. Indeed, until 1986 the Indonesian Institute of Aeronautics and Space (LAPAN) required NOAA data without atmospheric correction. It is even worse that local hardware constraints prevent any operational monitoring with mainframe computers. By analysing NOAA data with microcomputers, the methodology presented in this paper intends to fill this gap. It was tested with the study of large scale SST features in Indonesia from July 1981 to June 1985. Digital data were provided by digitizing 208 weekly SST charts of NOAA-NESS; with pixel size of 1°15' longitude and latitude. These data displayed a 0.5°K rms error as compared with 1985 in-situ measurements. Iterative and interactive factorial analyses combined with "parallelepiped" classifier, acting as a clustering technique, enhanced the SST spatiotemporal features. The study area was divided into zones in which pixels had similar SST profiles, whereas dates of occurrence of thermal anomalies were pointed out. Sea fronts and upwellings were mapped through spatiotemporal analyses of thermal gradients. This study stresses the possibility of an operational SST monitoring in Indonesia, allowing simple data manipulation with a type of hardware equipment maintained locally and easily.

* Dr. Gastellu-Etchegorry is a visiting professor at PUSPICS (Remote Sensing Center, Gadjah Mada University, Yogyakarta). Dr. Boely, an expert at ORSTOM (213 rue Lafayette, 75010—Paris, France) in oceanography and fishery, works at BPPL (Marine Fisheries Research Institute, Jakarta). Ir. Medellu is a staff member of IKIP in Manado.

INTRODUCTION

Nowadays it is becoming increasingly evident that a good knowledge of the physical characteristics of the oceans is necessary for better management of Earth's resources. Conventional techniques do not allow oceanographic surveys with sufficiently precise time and spatial resolutions. In this context, satellite remote sensing is becoming more and more common and a useful tool. Measurements over the oceans have been extensively used for weather forecasting, ship safety, and global scale studies of climate and sea conditions. Now, archival and current satellite data offer new opportunities for an operational management of marine activities. Remote sensing of Sea Surface Temperatures (SST) is the technique with widest impact. Even without complex calibration or atmospheric correction algorithms, there is a very good correlation between the radiometric levels racorded and the temperatures of the surface water observed. Moreover, sea water temperature is one of the easiest oceanic parameters to measure, if it is tolerable to restrict observation to the surface layer a few microns deep (Gastellu-Etchegorry *et al.*, 1983). The widespread distribution of remotely sensed thermal data is notable. Radiometers on various operational environmental satellites, e.g. the AVHRR of the NOAA polar orbiting satellites, currently supply SST measurements. Because these are transmitted with low transmission rates as compared to those of the Landsat and SPOT satellites, they can be acquired by inexpensive and simple ground stations. Thus, SST measurements from space are actually or potentially capable of making an important contribution to various scientific and economic marine activities.

Sea Surface Temperatures are one of the indicators of the evolution of oceanic water masses. In the case of climatology, small SST changes may indicate a significant change in heat energy storage within the ocean and may have a strong impact on atmospheric flow and weather patterns on large-scale basis, e.g. 10° longitude × 10° latitude. SST anomalies can produce significant variations in the circulation of the atmosphere (Robinson, 1985). Moreover, by acting strongly upon the rates of evaporation, SST influence greatly the creation and track of tropical cyclones. Another important application of satellite oceanography is fishery. This latter activity, due to the demand for food which increases daily, should be subject to much further development. However, this development is contingent on good management of the oceanic resources which exludes, for example, the occurrence of over-fishing. In Southeast Asia, fish catches are about 5.7 million tons whereas total potential yield is between 7.8 and 8.4 million tons (Chikuni, 1987). While most Asian marine fishing areas can contribute to still higher fish production, there are some spots within the region which have already shown signs of over-exploitation, such as the littoral of the Java Sea, the Gulf of Thailand, the western coast of India, and the Laguna Bay area in the

Philippines. In Indonesia where the 1984 marine fish catch was 1.5 million tons (D.J.P.. 1986). governmental planners expect fish productivity to increase significantly in future years.

Remote fishery assessment is assisted by measurement of some sea surface parameters which can affect distribution and abundance of certain fish species (Petit and Kulbicki. 1983). However. favorable physico-chemical factors do not always imply that fish are present. In order to be fully useful. these parameters must be available in near real time. Because fish responds to the total environment (Laevastu and Hela. 1970). their distribution cannot be attributed to any single parameter. Until now. most remote sensing studies have been conducted without complete suites of remote. conventional oceanographic. and fishing data. The common approach has been to investigate the relationship between a certain fish stock and a single remotely measured parameter such as temperature. salinity. chlorophyl. turbidity. or sea state. At present. expensive and complex remote salinity measurements. as applied to littoral and estuary fisheries. and to a lesser extent the remote assessment of chlorophyll as an index of basic biological productivity. are not fully operational. On the other hand. the relationship between remotely sensed temperatures and fish distribution (Pearcy. 1973) is already being commercially exploited. Migrating pelagic tuna fish appear during short periods within areas where there are significant gradients of temperature or/and other physico-chemical parameters. Some coastal pelagic fish migrate along the coasts and often follow the movements of sea fronts (Boely. 1979: Boely and Freon. 1979: Boely. *et al.* 1986) which vary in position according to the seasons and it can be monitored by satellite.

Upwellings and sea-fronts are among the main marine features which can be remotely detected with ease. Coastal upwellings are resulted from the drift of superficial waters due to the combination of topographic constraints with a wind field. Other oceanic upwellings are resulted from the divergence of surface currents in the open sea. In any case. they consist of cool waters. with a high content of mineral nutrients: which rise to the sea surface from lower aphotic oceanic layers. They constitute pockets of water. usually much colder than the surrounding waters. Their boundaries are indicated by an easily detectable narrowing of isotherms. The combination of light with mineral substances leads to a greatly increased production of phytoplankton. basic constituent of the food chain. followed by the development of zooplankton. The abundance of food. at all levels of the food chain. induces an increased production of living matter and thus large fish concentrations. These phenomena may be sporadic but usually they occur regularly with the seasons. They contribute to the richness of marine areas such as the littorals of Peru. Angola. Mauritania. and California. Sea-fronts are structures. usually more or less linear. which separate distinct water masses

with different temperatures or/and salinities. Important enrichment and subsequent increase of fish stocks take place in these mixing zones. Concentrations of fish which prefer one of the two water masses do not move in all directions.

The purpose of this study was to develop and validate a procedure for operationally monitoring the SST in Indonesia. This type of survey does not exist at this time. After a brief review of the main sources of error in determining remote SST, a methodology is defined for operational monitoring of SST with locally available hardware equipment. The procedure was tested with a study area (Figure 1) which includes all Indonesian seas (10°N to 15°S latitude, 90° to 140°E longitude); the time period extended from July 1981 to June 1985. Remotely sensed SST were validated with in-situ measurements. The use of an interactive clustering technique permitted the delineation of areas with homogeneous SST profiles and to stress when SST anomalies occur. It was

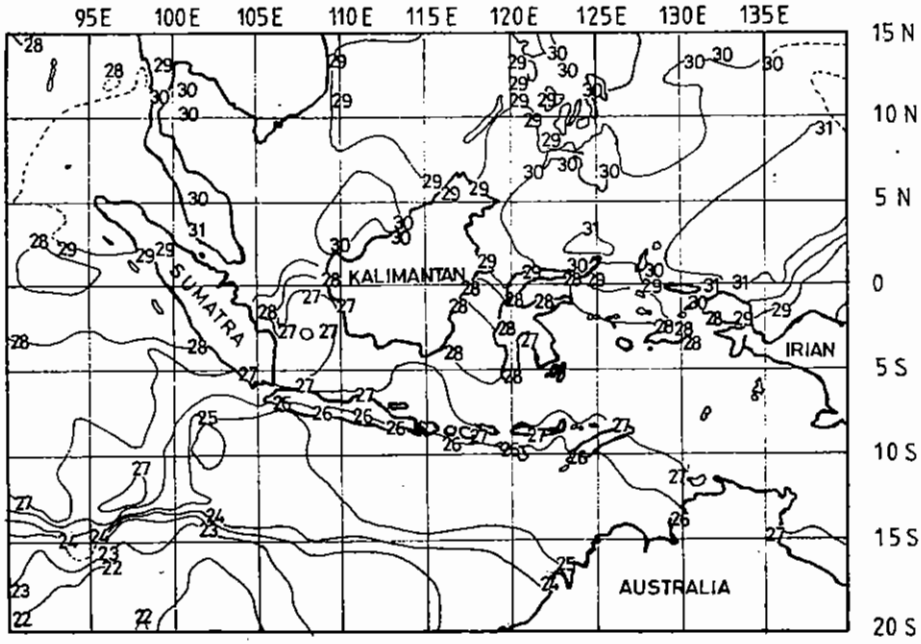

Figure 1. MCSST Chart of the Study Area, the 8/25/81.

Note: A sea front is present in the lower left corner.

followed by a systematic detection and analysis of thermal gradients; large sea fronts and upwellings are mapped.

THE REMOTELY SENSED DATA

Different physical and technological factors prevent the acquisition of SST by remote sensing as accurately as by in-situ measurement. For example, according to Planck's law, an error of only $(10)^{-3}$ in the sea surface emissivity introduces an error of about 0.07°K in the 12 μm thermal bandwidth. On the other hand, currently available spaceborne thermal infrared radiometers have an absolute calibration around 0.3°K. Another cause of inaccuracy stems from the fact that thermal electromagnetic radiation does not penetrate the sea surface, compared to radiation in the visible range, which prevents oceanographers from apprehending directly the marine vertical structure. Thermal remote sensing measures concern only the skin surface of the water. Radiations coming up from depths greater than 10 μm represent only 10% of the total heat flux arriving at the water surface (Gastellu-Etchegrorry *et al.*, 1983). Thus there is usually a negative temperature difference (0.1 to 0.5°K) between the remote sensed brightness skin temperature and in-situ measurements of the bulk temperature (Nicholls, 1979); oceanographers consider the top layer 50 cm deep, whereas usual ship routine measurements correspond to a layer extending from 2 to 5 m deep. The modeling of this temperature difference is very complex. It requires a knowledge of the surface wind speed, remotely sensed with a scatterometer, and of the local surface heat flux, which with present technology requires in-situ measurements.

Today the major source of error in determining the SST in cloud-free zones is caused by the interaction between the atmospheric constituents and the radiance which propagates from the ocean to the satellite. Within atmospheric windows, intervals of frequencies with no or low atmospheric absorption, this interaction is mainly due to water vapor and, to a lesser extent: aerosols, carbon dioxide, methane and ozone. In humid tropics, and so in Indonesia, atmosphere induces errors which may be larger than 6°K (McClatchey, 1976). In partly cloudy areas, it is also possible to estimate sea surface temperatures by using various techniques, e.g. the N-star technique which compares infrared radiances in contiguous pixels (Smith, 1968). In 1981, NOAA-NESS initiated an automatic correction of atmospheric errors with a multi-channel technique (MCSST) to derive operational SST products. The idea is that atmospheric absorption can be approximated to be linearly proportional to the radiant difference of simultaneous measurements at two different wavelengths (McClain, 1984). Buoy evaluations of MCSST values indicate a mean standard deviation of 0.6°K (Robinson, 1985). In

a country like a country like Indonesia. cloud cover is a particularly limiting constraint. During the mornings. the cloud cover tends to be less important but an important atmospheric veil is very often present. An all-weather survey requires the use of microwave radiometers. unfortunately. compared to thermal infrared sensors. their overall performance is poorer. both for spatial and radiometric resolutions. In totally cloudy areas. microwave radiometers provide SST with an accuracy of 2—4°K. During the next decade it is expected that SST will be obtained from space with an accuracy of 0.3°K. The along track scanning radiometer on board the ERS-1 European Space Agency satellite. due to be launched in 1989. is designed to meet this requirement.

The automatically area-averaged remotely sensed SST data allow a two dimensional synoptic view of all the oceans. with a high spatial resolution (1 km for the AVHRR of NOAA satellites): the maximum time repetitivity of data acquisition is 30 mn with the geostationary GMS satellite. and 12 hours with the polar-orbiting NOAA satellites. In Indonesia the National Institute of Aeronautics and Space (LAPAN) acquires and stores NOAA and GMS data on Computer Compatible Tapes (CCT). In this study. only NOAA data are considered due to the inadequate radiometric accuracy of GMS data. Before 1986 LAPAN. due to technological constraints. acquired only the channels 2 (0.725—1.1 μm) and 4 (10.3—11.3 μm) of the AVHRR radiometer on board NOAA satellites. which prevents any automatic atmospheric correction. Moreover. geometric corrections necessary for a multi-date analysis were not processed. Nevertheless. a comparison of these raw data with in situ measurements in the seram sea and Pacific Ocean (Boely *et al.*, 1986) displayed good local relative accuracies (less than 0.3°K) which allowed the detection of local thermal gradients. However. such data turn out to be useless for an SST monitoring over large areas and/or over different time periods. The display of a few NOAA data clearly emphasizes the importance of the cloud cover constraint in Indonesia. In order to get a repetitive survey of a large area. data from several consecutive days must be very often combined. At present. the local unavailability of reliable mainframe computer equipment. except in some governmental agencies. prevents any widespread processing of digital data stored on CCT magnetic tapes. and thus any operational SST monitoring. Even in LAPAN. the manipulation of a few CCT magnetic tapes for the search of thermal gradients may sometimes be a laborious task.

In this context. we have defined a procedure which is simple. but possibly operational in Indonesia. using a type of hardware which is locally available and well maintained: an Apple II microcomputer was chosen. In order to simulate the type of operational products that LAPAN is expected to provide soon. SST charts issued operationally by NOAA/NESS under the name MCSST (Multi-Channel Sea Surface Temperature) were ordered. The MCSST algorithm computes

an SST value at the intersection of each latitude/longitude grid line. Using this information, 1° isotherms having a spatial resolution of 100 km are plotted on sets of SST 1 charts. Although 1°SST data is available daily, these charts are generated once a week with the bulk of the data coming from the day before the date of generation. Due to the oceanic inertia, this weekly radiometric averaging does not induce a very important loss of information. In any case, this type of approach is necessary for zones with nearly permanent cloud cover. 208 MCSST charts, such as the one displayed in Figure 1, are required for a weekly survey of all Indonesian seas, between July 1981 and June 1985. In fact, due to cloud cover constraints, 8 charts are not available. In order to get an automatic data processing, all the MCSST charts are digitized. The digitization is manual, due to the unavailability of an automatic digitization system. Pixels are of a size (1°15′ latitude × 1°15′ longitude) slightly larger than the 1° gridded original MCSST. The study area is made up of 717 pixels (Figure 2). In the presence of several isotherms within one pixel, the accepted SST is the locally area-averaged SST. Each pixel is considered as a vector, or data file, with 208 temporal components (weeks). Then all data files are input into the computer memory; the temperature of pixel "i" during the week "j" being expressed as T(i,j). The unavailable information of the 8 missing MCSST charts is created with an interpolation algorithm.

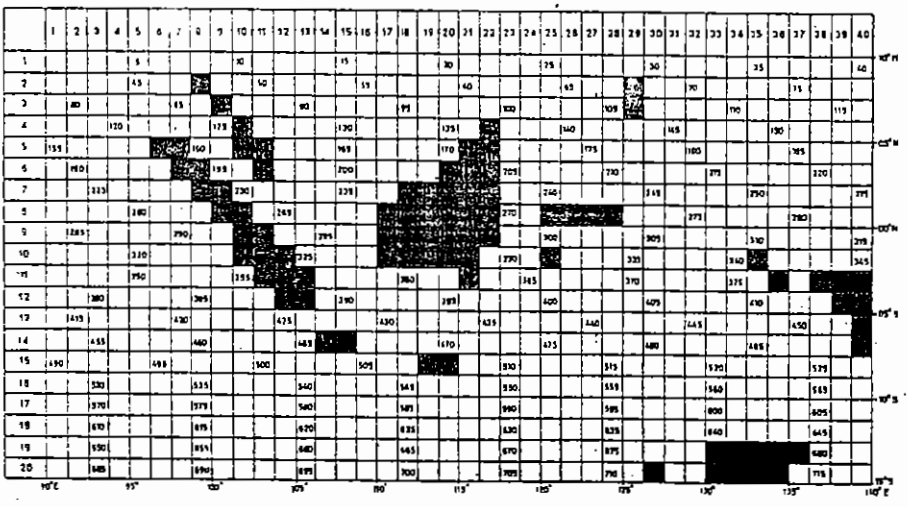

Figure 2. Digital Map of the Study Area

Note: Land areas are displayed as black areas.

LARGE SCALE SST PATTERN

Once all 717 temperature data files were entered into the Apple II, weekly and monthly charts were displayed. Figure 3 shows the SST distribution in October and November 1981. A southward move of warm waters begins in the Indian Ocean and a sea front can be noted perpendicular to the western coast of Sumatra.

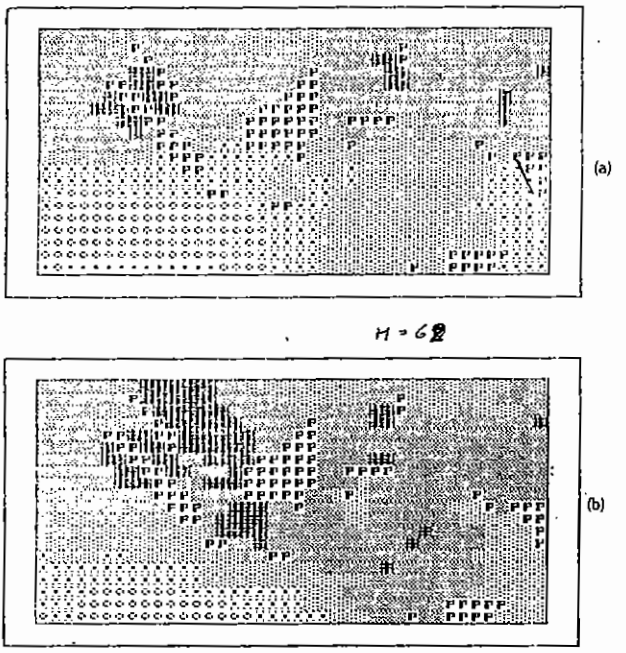

Figure 3. Monthly Mean SST in September (a) and October (b) 1981.
Note: Letters "P" denotes islands. Temperatures range from 26 C to 30 C (darker tones).

For oceanographic purposes it is interesting to analyse the temporal variation of the SST per pixel or per group of pixels. Latitudinal influence in the Indian Ocean can be analysed with the aid of the SST temporal profiles of pixels located at 95 East longitude and at different latitudes (Figures 4 and 5). As the latitude increases the mean SST decreases and the temporal SST variations are sharper and larger. Another example is provided by the analysis of the SST profiles of Figure 6: the sharp seasonal SST variations in December-January and

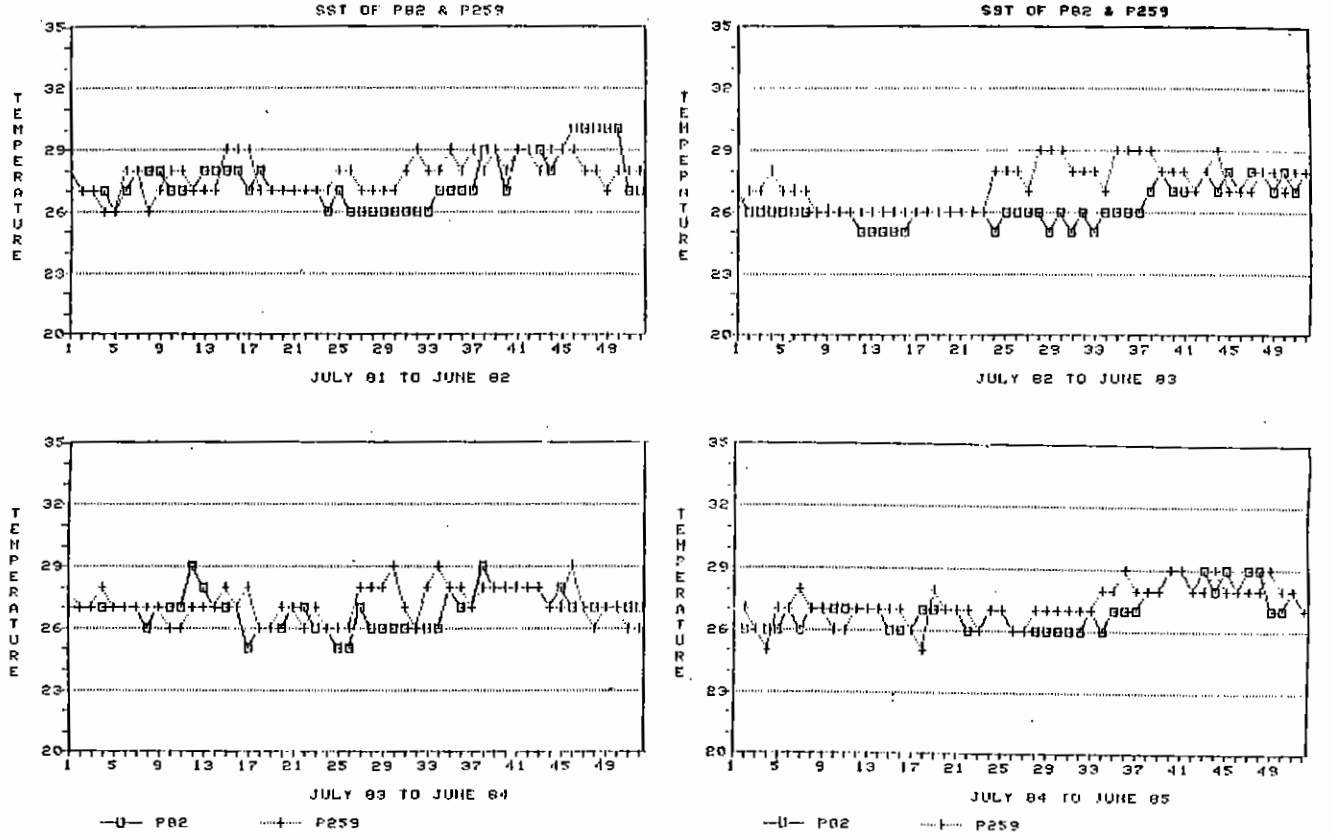

Figure 4. SST Temporal Profiles, with 52 Weeks per Year, of Pixels P82 (7°N) and P259 (1°N) at 93°E Longitude

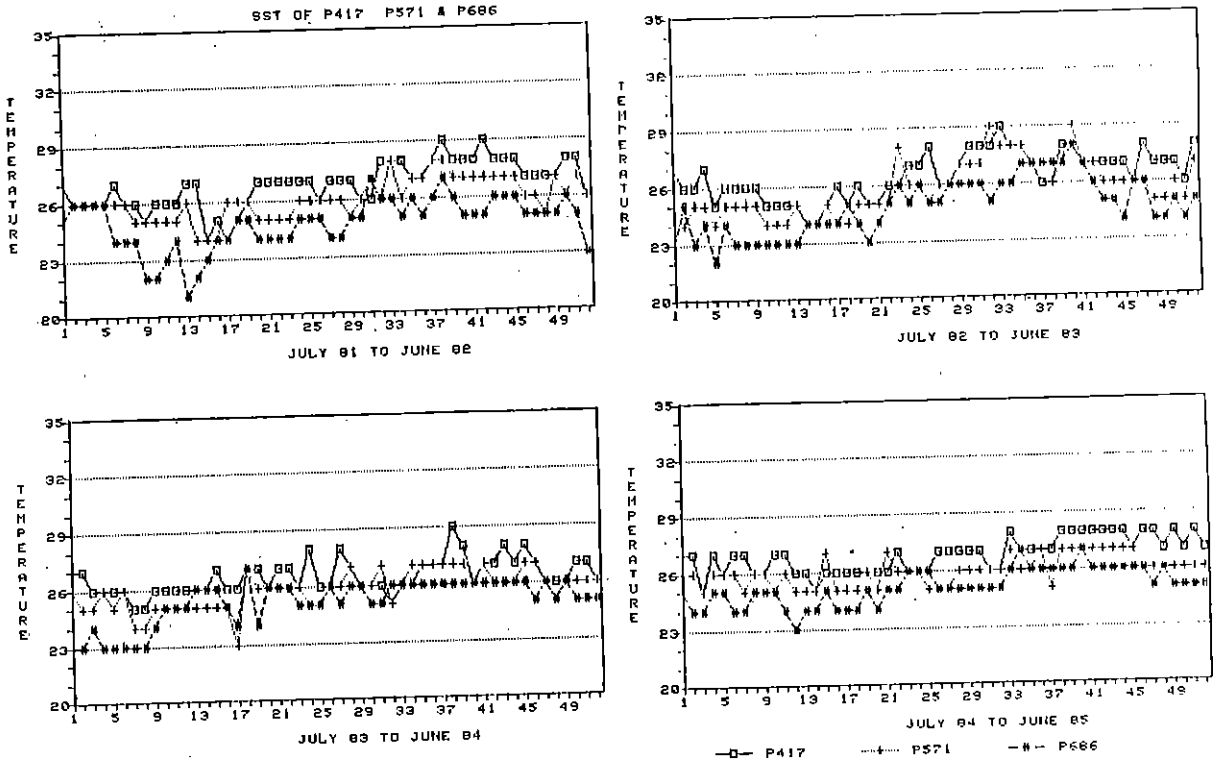

Figure 5. SST Temporal Profiles, with 52 Weeks per Year, of Pixels P417 (6°S), P571 (11°S) and P686 (15°S) at 93°E Longitude

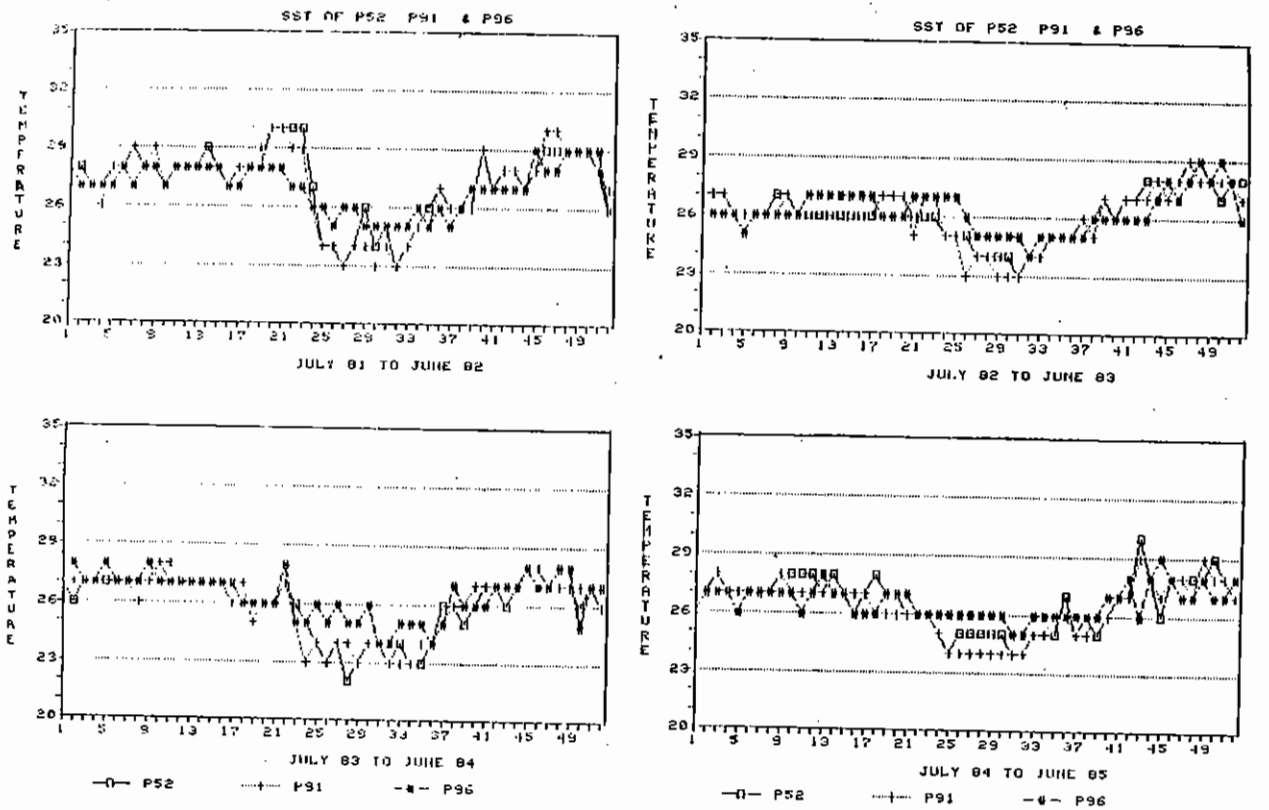

Figure 6. SST Temporal Profiles, with 52 Weeks per Year, of Pixels P52 (105°E, 8°N), P91 (107°E, 7°N), P96 (113°E, 7°N)

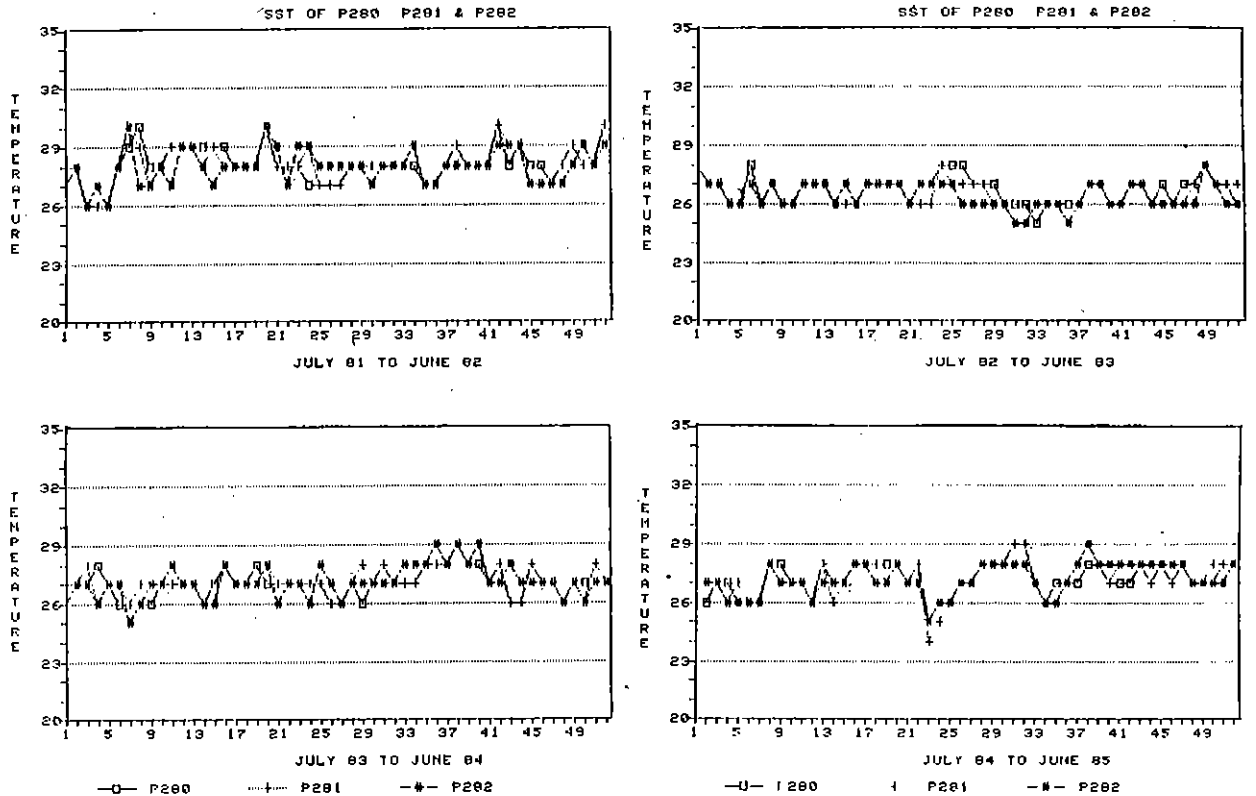

Figure 7. SST Temporal Profiles, with 52 Weeks per Year, of Pixels P280 (135°E, O°N), P281 (136°E, 1°N) and P282 (137°E, 0°N)

Note: Two occasional upwellings appear.

and March-April emphasize the occurrence of a sea front which corresponds to southward and northward movements of warm waters. Figure 7 displays the occurrence of an occasional upwelling around Biak, north of Irian Jaya in December 1984. These examples show the relevance of all the temporal SST profiles, however, due to their large number (717 × 208), they constitute a valuable but not easily readable product. In order to obtain a synthetic document, two parallel approaches were used to present information more efficiently: a spatial analysis which determines the homogeneous zones where pixels express similar SST profiles during a certain period, and a temporal analysis which stresses the time periods when SST anomalies occurred in a certain area. The notion of similarity between variables, either "pixel" or "time", was respectively expressed with the aid of temporal SST means and inter-time correlations. Because the grouping of pixels, within homogeneous zones, mainly took place with neighbouring pixels which had nearly equal SST means but which may not be very well correlated, the main decision parameter for similarity between pixels was the temporal correlation.

To determine the main temporal and spatial characteristics of the SST data, it was necessary to manipulate the 717 × 717 contigency table T(i,j). In the present study this is performed by an iterative and inter-active factorial analysis of correspondences (Benzecri, 1984) combined with a "parallelepiped" classifier. With some geometric and algebraic manipulations, this factorial analysis modifies the graphic presentation of a contigency table to gather most of the information within a limited number of graphics. In order to emphasize information about the similarity between the variables "pixel" or "time", the relative values and not the absolute values of the original data were considered. Because the analysis must be performed from the standpoints of both the variables "time" and "pixel", we required a distributional equivalence of these two types of variables. Thus, their relative values were computed with identical transformations, which correspond to different analytical transformations, which correspond to different analytical expressions. For the variables "pixel" the relative values are:

$$R(i,j) = T(i,j)/[T(i)*T]$$

with $T(i) = \sum_{j=1}^{J} T(i,j)$. $\quad T = \sum_{i=1}^{I} T(i)$. $\quad I = 717$, and $J = 208$

whereas, for the variables "time" the relative values are:

$$R'(i,j) = T(i,j)/[T(j)*T] \qquad \text{with } T(j) = \sum_{i=1}^{I} T(i,j).$$

In order to keep the distributional equivalence of the variables, the distance

between the points representing the variables was the Chi-square distance (Benzecri, 1984). For the variables "pixel", it is a usual Euclidian distance for which the relative data area individually centred in relation to the square root of "T(j)" and weighted with the inverse of "T(j)". The Chi-square distance between variables of the same type provides a quantitative measure of the similarity between these variables. For example, a very low distance between two "pixels" means that these two pixels express similar temporal SST, whereas a very low distance between two variables "time" means that all the pixels considered express similar SST profiles at the two times. Due to the speial characteristics of the Chi-square distance, the grouping of very close variables does not modify the distances between the other variables. Therefore no information is lost when grouping of variables takes place, and consequently no additional information is gaind if homogeneous groups of variables are indefinitely partitioned (Lagarde, 1983). Thus the new spatial and temporal variables are respectively:

$$Z(i,j) = R(i,j)/\sqrt{T(j)} - \sqrt{T(j)} \qquad \text{with a weight } T(i)$$

and $$Z'(i,j) = R'(i,j)/\sqrt{T(i)} - \sqrt{T(i)} \qquad \text{with a weight } T(j)$$

The inertial momentum of the Z(i,j) and Z'(i,j), expressed with the help of the covariance matrix $[Z(i,j) \times \sqrt{T(i)}]$, are equal. In order to determine the axes for which this inertial momentum is maximized, the eigen values and eigen vectors of the covariance matrix are computed. The projection of the Z(i,j) on the new axes defined by the eigen vectors gives the new coordinates of the variables "pixel", whereas the new coordinates of the variables "time" are given by the projection of the Z'(i,j). Eigen vectors, from the first to the last, provide uncorrelated information which represent decreasing percentages of the original information: the total original information is given by the 208 factorial axes. Thus, two-dimensional displays with the first two eigen vectors as axes, visualize the main spatial and temporal trends of the SST data. However, in the case of original data which are too complex, such trends may be very confused. For example, let us consider a factorial analysis of the SST of all the study area during four years. Mainly because thermal characteristics of neighbouring pixels vary slightly, the information provided by the two first factorial axes represents only 25 percent of the total original information. As a result, the visualization of the 208 variables "time" and of the 717 variables "pixel" is very confusing. This poor discriminating power is due to the fact that the diagonalisation of the covariance matrix maximizes the total variance of all the equalized variables, and not the variances of individual groups of similar varibles. This problem could be solved automatically with a clustering technique combined with a canonical analysis (Schowengerdt, 1983), or by considering a number of factorial axes large enough to obtain a high percentage of information.

Due to experimental constraints, essentially the small computer memory capacity, an intermediate approach is chosen, with only limited numbers of pixels (fewer than 200) are analyzed at a time. In the first step, an example of application of the factorial analysis of correspondences is provided for the study of variables "time". Figure 8 displays all variables "time" after the factorial analysis of a set of pixels located in the South of Bali, within a graph defined by the first two eigen vectors. The displayed information represents 62% of total information. Most variables are centred around the origin of the graph. The visualisation of the SST temporal profiles (Figure 9) of some pixels confirms the hypothesis that most variables located outside the central part of the graphic of Figure 8 represents dates of appearance of SST anomalies. The number of consecutive ex-centred variables "time" indicates the duration of the SST anomaly. The seasonal aspect of the anomaly is stressed by the constancy of the time gap (50—60), 52 being the number of weeks in a year, between the different groups of consecutive variables "time". In the present case the SST anomaly is a seasonal upwelling which occurs during the months of July and August. Thus, for a given area the factorial

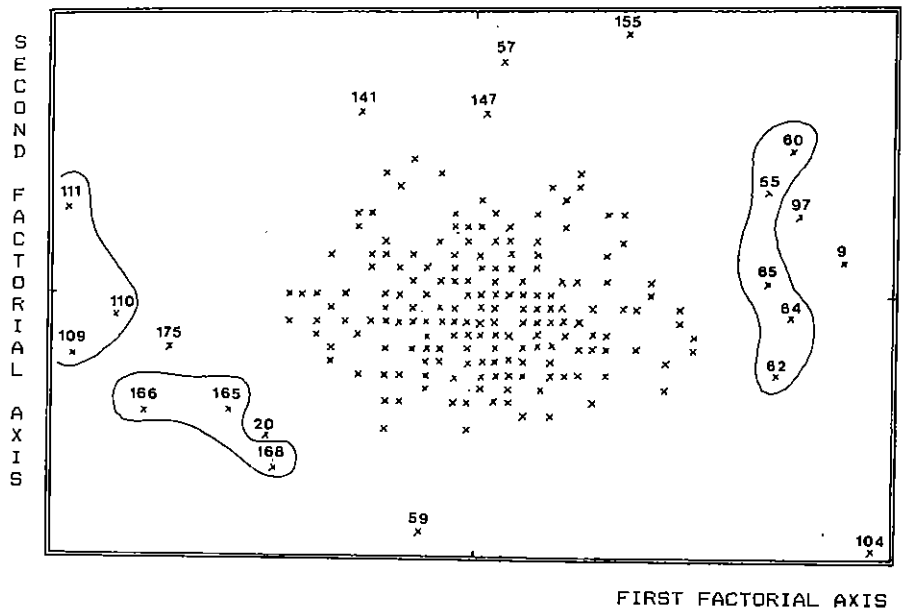

Figure 8. Variables "time" after a Factorial Analysis of 40 Pixels, South of Bali.

Note:

Ex-centred variables indicate dates of SST anomalies. Groups of consecutive dates are outlined. The plot represents 62% of information in the data set.

analysis. from the standpoint of the variables "time". permits an immediate assessment of dates when SST anomalies occur. However. it must be remembered that the area considered must not be too large in order to permit the display of non confused two-dimensional information.

The determination of the large scale SST pattern is processed by partitioning the study area in sets of pixels which are successively analysed with the aid of a factorial analysis combined with a classification. Figure 10 displays. within a graph defined by the first two eighen vectors. the results of the analysis of a set of pixels located south and north of Java. Well discriminated pixels have very different SST profiles. but mixed pixels may have similar or different SST profiles: indeed the displayed information represents only 51 percent of the original information. In order to improve the analysis. the information provided by the third and fourth factorial axes is also considered. With the aid of the Chi-square distance. and by taking into account the respective levels of information provided by the first four factorial axes. a classification is performed with the aid of a "parallelepiped" classifier (Gambart. 1983). Due to the strong negative correlation between the value of the Chi-two distance and the value of the inter-pixel thermal similarity. the classes correspond to contiguous geographical areas. A class is called a homogenous zone if it includes a sufficiently important number of pixels. and if it is far enough from other classes. Six classes are outlined in Figure 10. All the pixels which belong to a group are located in the same marine area: zones 16 and 21 correspond to the west and east part of Java Sea. whereas zones 17. 18. 19 and 23 correspond to marine areas south of Java. from west to east. Some pixels are not attributed to a group: such as the case for pixel (504). and pixels (538. 548) which belong to groups not included in the presently analysed set of pixels. The following step of the study consists of the factorial analysis of sets of pixels of overlapping areas. Such an approach permits the grouping of pixels and classes which belong to sets of pixels successively analyzed. but which are characterized by similar SST profiles. During the classification. a trade-off is performed to combine the accuracy of the results (large number of classes) and the required reduction of data input. An SST temporal profile is defined for each class. as the mean SST temporal profile is defined for each class. as the mean SST temporal profile of all the pixels within this class. If the correlation between one class and its pixels is less than 80%. then this class is again processed. When a pixel. such as pixel (504) in Figure 10. cannot be attributed to a class. it is said to belong to an intermediary zone. Finally. after several interactive iterations. most pixels are classified in 40 classes. called homogeneous zones (Figure 11). This type of document is revealed to be very useful for oceanography. especially in order to understand better the large scale SST distribution in Indonesia. For example. by considering time periods longer than 4 years it would be very interesting to study the

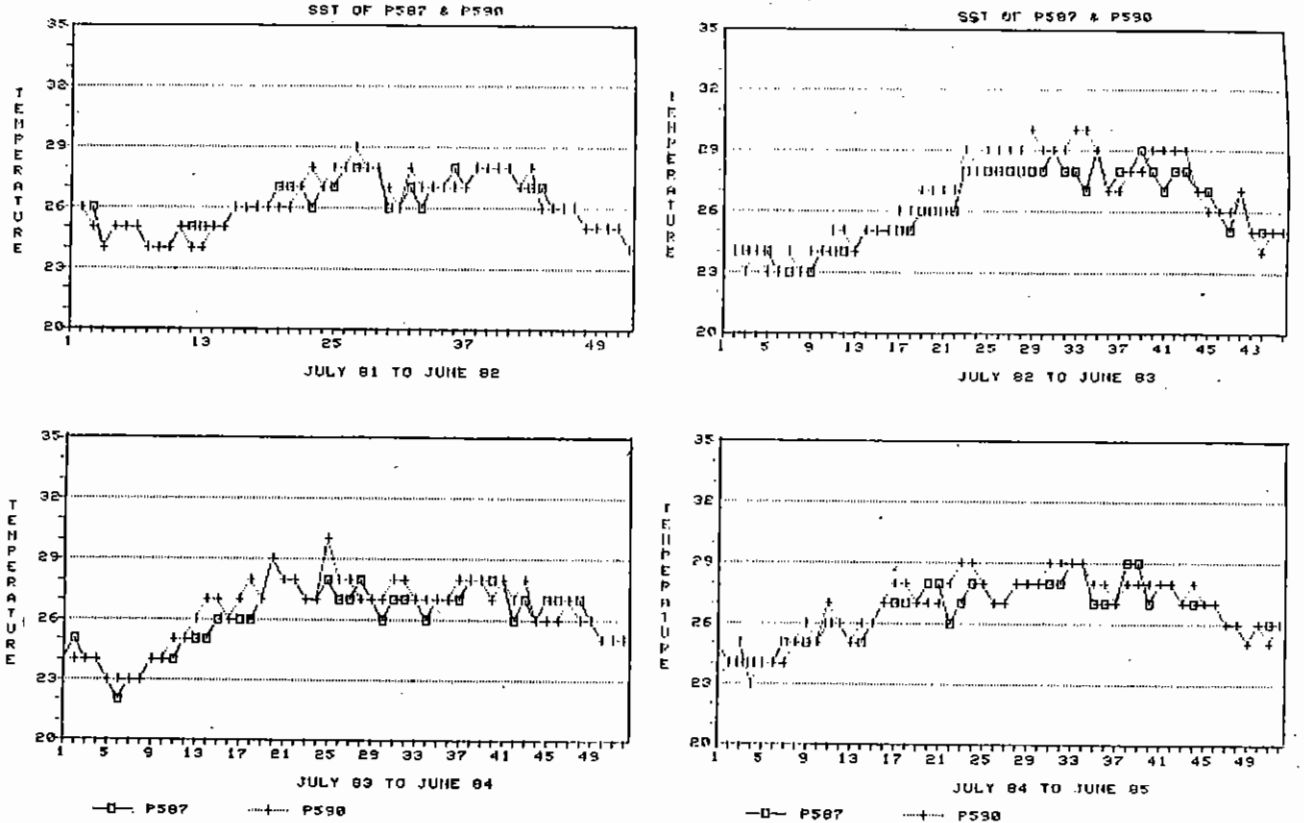

Figure 9. SST Profiles of 2 Pixels, South of Bali.

Note: The presence of a seasonal SST anomaly, for dates ex-centred in Figure 8 is verified.

temporal variability of these zones.

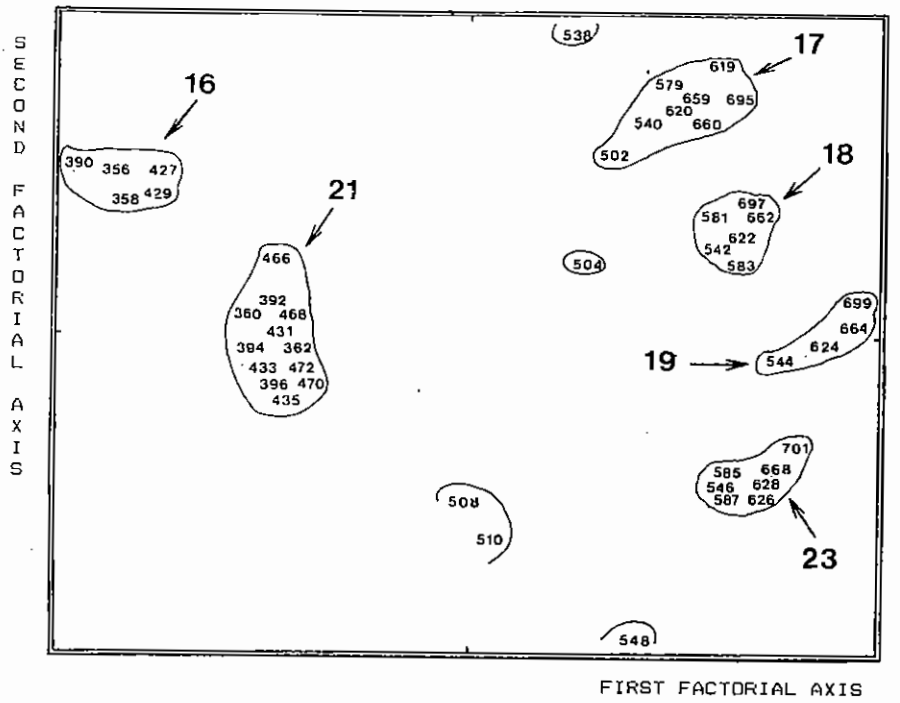

Figure 10. Variables "pixel" after a Factorial Analysis of Pixels, South of Bali.

Note:
The outlined groups of pixels correspond to pixels with similar SST profiles; they belong to the same class.

Detection of Upwellings and Sea Fronts

As has already been mentioned, the detection of upwellings and sea fronts is a very useful task for many oceanographic activities, and especially for fisheries. In the present study, their occurrence is supposed to be revealed by sudden SST changes of one or several pixelsl to neighbouring pixels. Different approaches can be used to detect and enhance these SST gradients. A simple but effective technique consists of combining high-pass spatial filtering and SST gradient thresholding. Spatial filtering is a pixel by pixel transformation of an image which depends not only on the SST value of the pixel being processed but also on the SST values of neighbouring pixels. It is a context-dependent operation that alters the SST value of a pixel according to its relationship with the SST values of other pixels in the immediate vicinity. High-pass filtering enhances detail in an image at

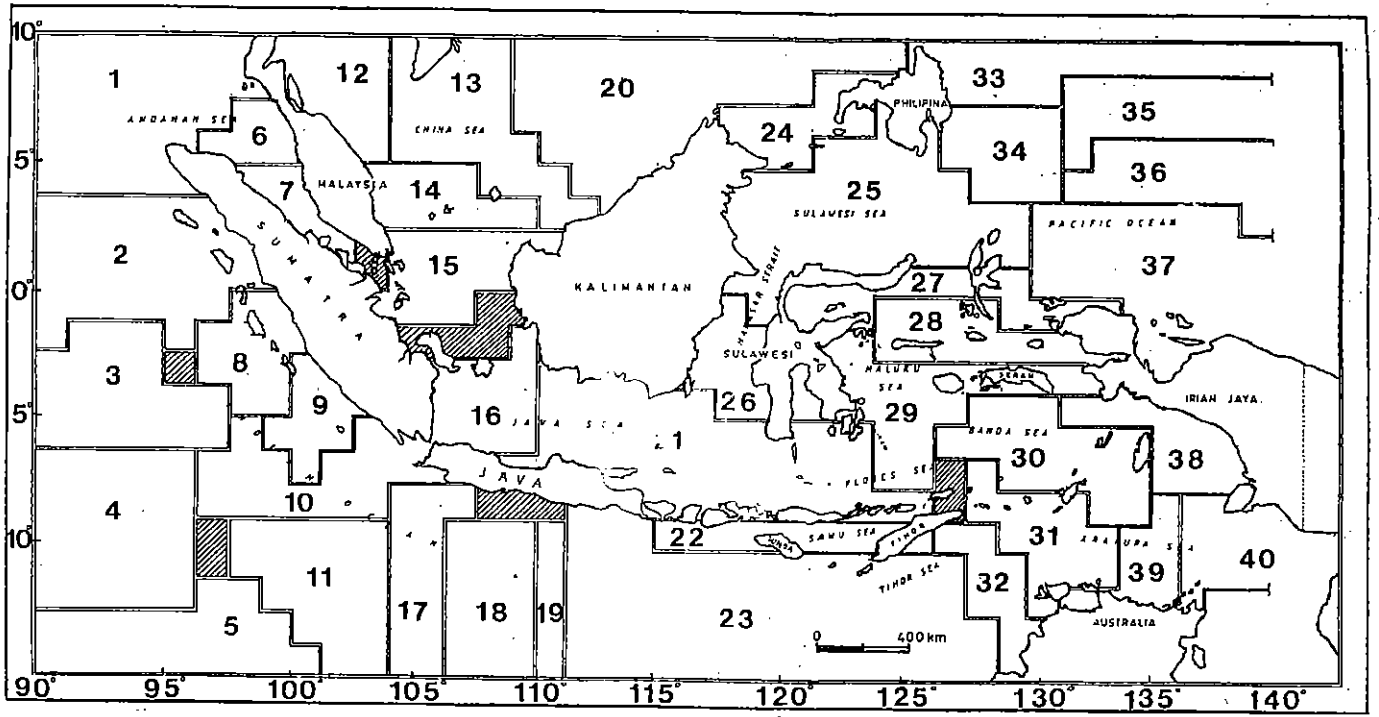

Figure 11. Map of Homogeneous Zones with Similar SST Profiles

the expense of large area SST information. It can be implemented with the convolution of a function, called Point Spread Function (PSF) in optical terminology, which can be displayed as a matrix having a positive weight for the processed pixel within the input image, and negative weights for surrounding pixels. This filtering is usually represented by a window, Q × Q pixels large, moving through the original image. The convolution which transforms the pixel P(i,j) into the output pixel P′(i,j) processes the pixels P(a,b) within the window centered around P(i,j); it can be written:

$$P'(i,j) = \sum_{a=i-Q/2}^{i+Q/2} \sum_{b=j-Q/2}^{j+Q/2} P(a,b).PSF(i-a, j-b)$$

If the width of the input image is M pixels by N lines, the number of mathematical operations, and thus the computation time required to create each output pixel is proportional to Q × M × N. Thus, with a micro-computer the study of a large set of pixels must be processed with small moving windows. With a linear spatial transformation, as in this study, input pixels within the window are multiplied by the corresponding PSF values (weights) and then summed to create each output pixel. The window moves successively over every pixel in the same line, for all lines.

Sea fronts, inl contrast to upwellings, are often characterised by spatiotemporal SST gradients according to a predominent direction. In this context the search and enhancement of SST gradients must be directional. This is achieved by filtering the original SST values in two orthogonal directions, e.g., horizontally and vertically, and combining the results in a vector calculation. The magnitude and direction of the local SST gradient is given by the length and direction of the composite vector. Due to the large sizel of the pixels (1°15′ longitude and latitude), small moving windows (2 × 2) are considered. However, in the case of pixels with a smaller size, and according to the aim of the study, larger moving windows may be considered (Pratt, 1978). Sharp SST gradients are easily emphasized on displays by applying a threshold to the gradient image. These displays can be processed for weekly, monthly or yearly data. Figure 12 displays the most important latitudinal SST gradients during the first two weeks of October 1981. These periods correspond to a southward movement of warm waters to the southern hemisphere. This type of information is an enhancement of the original information (Figure 3); the presence of the southern sea front in the Indian Ocean is easily verified with the SST profile of pixel P686 (Figure 5). Figure 13 displays the position of the main sea fronts and upwellings during the four years of the study. They were discovered by enhancing and thresholding spatiotemporal SST gradients. Some SST features were already mentioned in this paper: sea fronts located in the south Indian Ocean (Figure 4) and in the South China Sea (Figure 5), and the large upwelling zone in the south of Bali and Java (Figure 9).

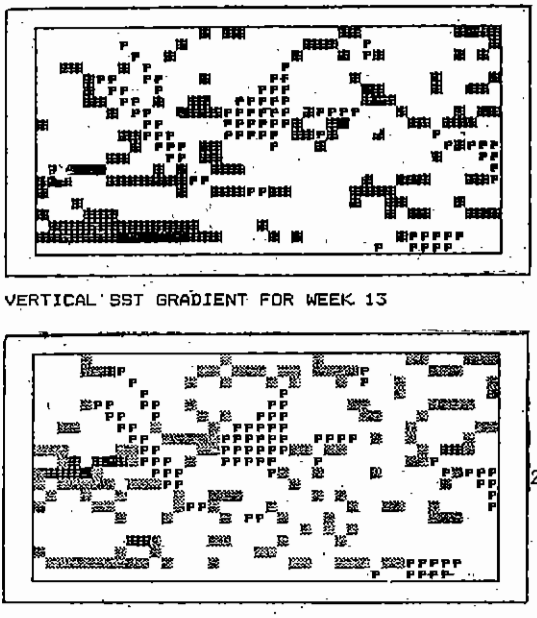

Figure 12. Location of Main Vertical SST Gradients during the First Two Weeks of October 1981

Note:
The presence of the sea front located in the lower left corner is verified with sharp SST gradients during weeks 13 to 17 of P686 (Figure 4).

CONCLUSION

Detailed results obtained with the present methodology will be given in a future publication. In a first approach, with simple computer equipment locally available and easily maintained, this procedure provides easy and quick descriptions of oceanic conditions within the Indonesian Archipelago. In this region, the marine seasons which are mainly influenced by alternate moonsons are poorly known in spite of the general description of Wirkty (1957, 1961), which is still valid. The present methodology allows us to improve our knowledge of the different marine seasons. Also it enables us to apprehend quickly the spatial and temporal interannual and seasonal variations of the marine climate on large areal extents (Figure 12). Due to its position on both sides of the equator, the Indonesian Archipelago has an oceanic climate with large interannual variability.

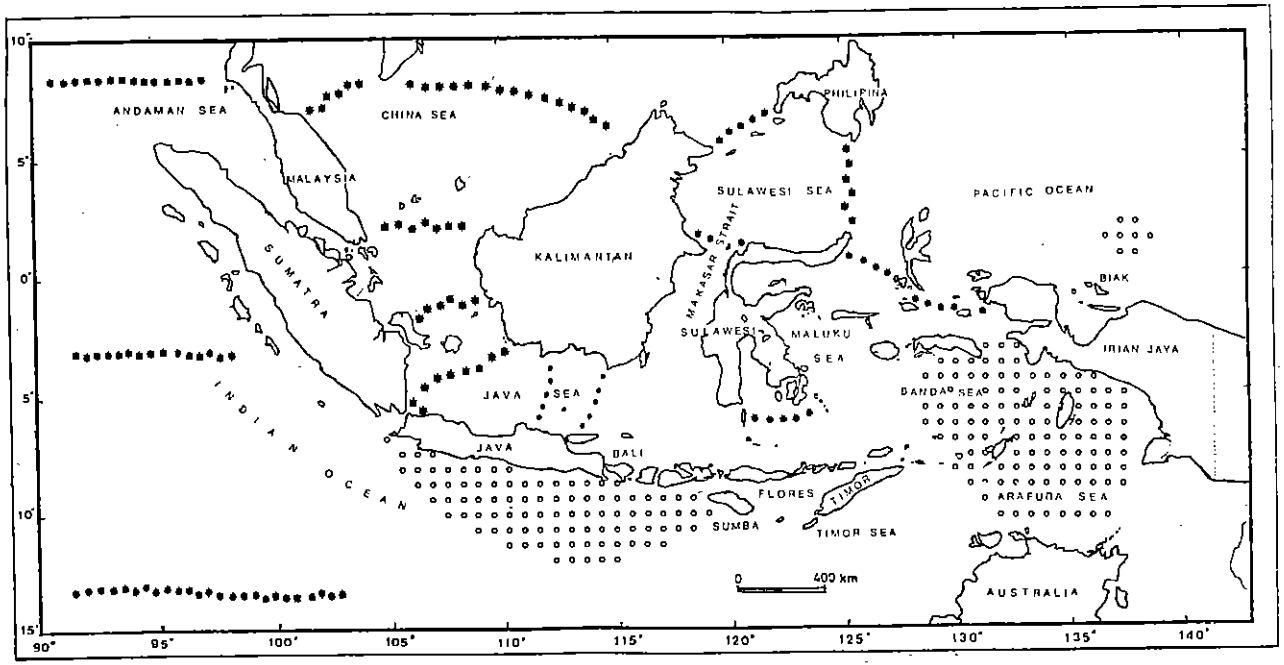

*Figure 13. Main Sea Fronts (* * *) and Seasonal Upwellings* (ooo) *between 1981 and 1985*

Note:
A non seasonal upwelling around Biak is also shown. This display results from an enhancement of a four year average of vertical and horizontal SST gradients.

Seasonal variations are usually less important. They depend on the interannual variability. They can also be influenced by specific local conditions that may be indirectly analysed through the detection of marine seasonal SST variations as the example in Biak (Figure 7) shows.

The detection and monitoring from space of the marine phenomena previously mentioned is quite important both from theoretical and practical viewpoints. Thus, for fishery the behaviour of some fish species, usually pelagic, may be greatly influenced by the global movement of the water masses. Their presence and subsequent fish production often depend on marine seasons. Climatic lengthenings or shortenings of the fishing season lead to considerable gains or lossses. In the same way, fish stocks may avoid an usual fishing area due to the occurrence of a climatic anomaly which may be detected quickly thorough remote sensing. We can envisage a systematic determination of the spatial, time, and temperature ranges of particular phenomena, like upwellings and sea fronts, which usually induce marine enrichment and a subsequent increase of important age groups (Boely, 1979: Boely and Freon, 1979: Boely *et al.*, 1986). Presently the analysis of the SST spatial and temporal evolutions in Indonesia can have only a partial role because relationships between the marine environment and the abundance of fish species must be first better defined. This approach requires a better knowledge of the biology of the fish species concerned. Then, remote sensing will no longer be merely descriptive but will provide an efficient tool for a real-time monitoring of fish stocks. Moreover, it will allow experts to forecast the probable locations and dates of appearance of large concentrations of fish stocks, and thus will be valuable for planners.

Fishery is only one of the applications of the methodology which has been presented. General climatology is another important example. Indeed, surface temperatures are indicators of the water masses which may succeed each other in a given position, and which exert significant influence on the whole earth's climate. In the long run there is a perpetual interaction between the marine and terrestrial domains, especially in Indonesia just as there are in other parts of the world, notably the littorals of peru and Ecuador where presence or absence of seasonal currents may completely alter sesonal configuration. Although these currents are considered as the main cause of many changes, they are only the indication of an important modification of the tropical and equatorial oceanic system at the level of the Pacific.

The present methodology successfully detected the main seasonal and interannual SST features (sea fronts, upwellings) in the Indonesian Archipelago. It is intended to fill a gap during the next few years, in Indonesia. During that time, it will permit operational SST monitoring for fishery and climatology. Due to the present constraints, the following procedure is proposed. Once automatic

atmospheric and geometric corrections are processed by LAPAN, digital data on CCT magnetic tapes are formatted to allow their transfer to potential users, such as the BPPL (Marine Fisheries Research Institute), who can process them with micro-computer systems, which in contrast to main-frame computers are easily available and maintained in Indonesia. For oceanographic applications which do not require a small spatial resolution, the process of area averaging in LAPAN may reduce greatly the volume of data, and thus may ease digital processing without significant information loss. This type of readily useful information is expected to be soon operationally supplied by LAPAN.

REFERENCES

Benzecri, J.P. *et al.* 1984. *L'Analyse des Donness.* Paris: Dunod.

Boely, T. 1979. *Biologie des 2 especes de sardinelles (Sardinella aurita et Sardinella maderencis) des cotes Senegalaises.* Doctorat d'Etat, Universite Paris VI, p. 286.

Boely, T. and Freon, P. 1979. Les ressources pelagiques cotieres. *FAO, Doc. Tech. Peches.* 186.1.

Boely, T. *et al.* 1986. *An Evaluation of the Abundance of Pelagic Fish around Seram and Irian Jaya (Indonesia).* ORSTOM, Etudes et Theses.

Chikuni, K. 1987. Potential Yield of marine resources in Southeast Asia. *Symp. on the Exploitation and Management of Marine Fishery Resources on Southeast Asia.* Darwin, 16—19, Feb. 1987.

D.J.P. 1986. *Fisheries Statistics of Indonesia-1984.* Jakarta: Direktorat Jenderal Perikanan, Departemen Pertanian.

Gambart-Ducros, D. 1982. *Texture et Teledetection.* Toulouse: Rep. CESR.

Gastellu-Etchegory, J.P., and Pramono Mardio. 1983. The Remote Sensed Sea Surface Temperature: a case study in Indonesia. *Ind. Jour. Geog.*, 13 (46):13—28.

Laevastu, T., and Hela, I. 1970. *Fisheries Oceanography.* London: Fishing News LTD.

Lagarde, J. 1983. *Initialisation a L'analyse des donnees.* Paris: Dunod.

McClain, E.P. 1984. Multi-channel Sea Surfaces Temperatures from the AVHRR on NOAA-7. Satellite derived SST: Workshop II, Pasadena, Ca. *JPL Pub* 84—5:1—8.

McClatchey, R.A. *et al.* 1976. *Atmospheric Transmittance from. 25 to 28.5 μm.* Supplement Lowtran 1976. AFGL-TR-76-025B.

Nicholls, S. 1979. Intercomparisons between the MRF Hercules and Surface

Observations from the JASIN Meteorological Ships. *Jasin News*. 19:9-11.

Pearcy, W.G. 1973. Albacore Oceanography of Oregon. *Fish. Bull.* 71 (2):489—504.

Petit, M., and Kulbicki, M. 1983. Radiometrie aerienne et prospection thoniere dans la zone economique exclusive de la Polynesie Francaise. *Oceanographie*. No. 20.

Pratt, W.K. 1978. *Digital Image Processing*. New York: John Wiley and Sons.

Robinson, I.S. 1985. *Satellite Oceanography*. England: Ellis Horwood Limited.

Schowengerdt, R.A. 1983. *Techniques for Image Processing and Classification in Remote Sensing*. London: Academic Press.

Smith, W.L. 1968. An Improved Method for Calculating Tropospheric Temperature and Moisture from Satellite Radiometer Measurements. *Month. Weath. Rev.* 96:387—396.

Wirtky, K. 1957. Die Zirkulation an der Oberflache der sudotasiatischen Gewassez. *Deut. Hydrogr. Zeit.* 10.1.

Wirtky, K. 1961. Physical Oceanography of the Southeast Asian Waters. *Naga Rep.*, 2.